

Synthesis and characterization of carbon microspheres from rubber wood by hydrothermal carbonization

Tanveer Ahmed Khan,^a Hyun-Joong Kim,^{a*} Arun Gupta,^b Saidatul S Jamari^{b*} and Rajan Jose^c



Abstract

BACKGROUND: Carbon is the raw material for many commercial products; conventionally their production is from non-renewable sources such as petroleum coke, pitch and coal. Recently carbon has been obtained from bioresources because of their renewability and high lignocellulosic content. This article details the synthesis of carbon microspheres from rubber wood, which is one of the largest commodity plants, via hydrothermal carbonization (hydrothermal rubber wood carbon; HTRW carbon) and evaluation of their characteristics.

RESULTS: Two sets of carbon were synthesized: (i) in the first set, excess of water (20–40 × weight of biomass) was used in the hydrothermal process at 180–260 °C for 3–9 h; and (ii) in the second set, water ratio was 25–35 × weight of biomass and the hydrothermal carbonization (HTC) reaction temperature was fixed at 260 °C. The H/C and O/C ratios of starting rubber wood were ~1.78 and ~0.85, respectively, which upon processing through the first strategy resulted in H/C ~0.78 and O/C ~0.29; thereby suggesting increased condensation under HTC. On the other hand, the carbonization process was accelerated by water when the temperature was maintained at 260 °C; Fourier transform infrared (FTIR) studies show that this carbon has a different chemical structure from the starting rubber wood. Scanning electron microscopy (SEM) images showed that HTRW carbon was in the form of microspheres (size ~1.5–5 μm).

CONCLUSION: HTRW carbon with carbon content as high as 68% was developed from rubber wood biomass by hydrothermal processing of a mixture containing 35 times more water than the solid raw biomass at a temperature of 260 °C for 7 h.

© 2018 Society of Chemical Industry

Supporting information may be found in the online version of this article.

Keywords: hydrothermal carbonization (HTC); carbon content; hydrothermal rubber wood carbon (HTRW carbon)

INTRODUCTION

Biomass is a sustainable source of many industrial raw materials including cellulose and carbon, and is anticipated to represent >70% of the aggregate viable energy source supply by 2030.¹ Plant biomass is rich in lignocelluloses, therefore, appropriate for production of highly value-added bio-products such as carbon and cellulose.² Furthermore, conversion of biomass into carbon has emerged as an attractive alternative to traditional sources such as petroleum coke, pitch and coal.^{3,4} A significant part of the biomass was utilized as a fuel in past decades, causing the emission of greenhouse gases such as CO₂, SO₂, and so on. Recently, developing functional materials from renewable sources such as biomass has become of paramount importance due to the depletion of natural resources and to eliminate or discourage widespread mining for life-sustainability.⁵ Furthermore, the biochars produced from biomass feedstock have higher carbon content and, therefore, offer a larger heat capacity.^{5–8}

Hydrothermal carbonization (HTC) is a simple biomass carbonization process, which offers many advantages such as generation of carbon at lower temperatures (<250 °C) than that required

for other carbonization protocols such as ignition, pyrolysis, and gasification.⁹ During HTC, biomass is processed in hot pressurized water, excluding the energy intensive pre-drying step.¹⁰ The products from HTC include hydrochar, a liquid fraction, and gases as a result of hydrolysis, dehydration, decarboxylation, aromatization, and re-condensation responses.¹¹ Hydrochar is the main yield

* Correspondence to: H-J Kim, Lab. of Adhesion & Bio-Composites, Program in Environmental Materials Science, Research Institute of Agriculture and Life Sciences, Seoul National University, Seoul 151-921, Republic of Korea, E-mail: hjokim@snu.ac.kr; or SS Jamari, Faculty of Chemical and Natural Resources Engineering, Universiti Malaysia Pahang, 26300 Kuantan, Pahang, Malaysia. E-mail: sshima@ump.edu.my

a Lab. of Adhesion & Bio-Composites, Program in Environmental Materials Science, Research Institute of Agriculture and Life Sciences, Seoul National University, Seoul, Republic of Korea

b Faculty of Chemical and Natural Resources Engineering, Universiti Malaysia Pahang, Kuantan, Malaysia

c Faculty of Industrial Science and Technology, Universiti Malaysia Pahang, Kuantan, Malaysia

with high carbon content, is grindable, and shows hydrophobicity properties. The liquid fraction is considered as a derivative stream containing numerous profitable natural chemicals, for example, furfural, hydroxymethyl furfural, lactic acid, formic acid, and levulinic acid.^{12–14} The HTC procedure is grouped into (i) low temperature HTC (~250 °C) and (ii) high temperature HTC (300–800 °C) based on the heating temperature and the final product. The low temperature HTC is a single-step environment-friendly process applicable to a diverse range of biomass for their carbonization. Low temperature HTC is similar to the natural coalification process, but is very fast, typically taking just a few hours, compared with the latter that takes millions of years.¹⁵

Woody biomass has three principal components, hemicellulose, cellulose, and lignin, and their ratios are different in different biomasses. Chemically hemicellulose is a hetero-polymer comprising different mono-saccharides together with pectinose as well as xylose; cellulose is a poly-saccharide made up of glucose; and lignin is a phenolic polymer. The relative constitution of these three components in biomass influences the carbon yield during an HTC process. Despite the advantages of HTC in converting raw biomass into carbon, only a few papers have discussed the relative conversions from various components (i.e. hemicellulose, cellulose, and lignin);¹⁶ most importantly biomass interactions with water and the mechanistic details of biomass conversion into carbon during the HTC process are not clearly understood.¹¹

Raw biomass would be a cheaper alternative to high cost precursors such as cellulose, lignin, sugar, etc. to manufacture carbon through HTC. In this context, rubber is one of the largest commodity plants, and its wood has been developed as one of the most viable raw materials for many applications such as furniture, construction materials, and wood-based composites. Rubber is a fast-growing plant, however, rubber wood fibers have relatively low strength such that their durability is limited. Alternatively, rubber wood could be an excellent carbon precursor because of its high content of cellulose, hemicellulose, and lignin.¹⁷ To the best of our knowledge no study has so far reported the use of rubber wood fiber to produce carbon. In the present work, we investigate the potential of rubber wood fiber as precursor for the production of carbon via an HTC process emphasizing the mechanistic details of the interaction of wood with water. The rubber wood produced via hydrothermal carbonization is termed hydrothermal rubber wood carbon (HTRW carbon) in this article. The HTRW carbon showed microsphere morphology and their chemical as well as structural characteristics are systematically studied and reported.

EXPERIMENTAL SECTION

Materials

The rubber wood fibers were obtained from Robin Resources Sdn. Bhd. Malaysia. The samples (denoted as biomass) were kept in an oven overnight at 105 °C to remove moisture until constant weight was reached.

Carbon syntheses

The HTC experiments were conducted in two sets in a 2.1 L buchi-glasuster stainless steel autoclave. In the first set of experiments, 50 g of oven dried sample (biomass) was immersed in water (biomass to water ratio varied from 1:20 to 1:40 w/w) and stirred for 4 h at room temperature, and subsequently transferred to the autoclave and heated to between 180 and 260 °C at a heating rate of 5 °C min⁻¹ for 3–9 h. In the second set of experiments, water

content was ~25–35 × weight of biomass and the HTC reaction temperature was fixed at 260 °C for 5–7 h. After each reaction, the reactor was cooled down to room temperature and the solid part was separated through filtration. The filtrate was washed repeatedly using distilled water and subsequently dried at 105 °C for 24 h (denoted as the hydrochar).

Sample characterization

To quantify the carbon transformation by the hydrothermal process, an elemental (carbon, hydrogen, nitrogen and sulphur) analysis was carried out using the German made Vacro Macro Cube, S/N-2012/1005. The phase and structure of the carbon were studied by X-ray diffraction (XRD) technique using Rigaku miniflex II (RGS Corporation Sdn Bhd, Selangor, Malaysia) X-beam diffractometer employing Ni-filtered CuK α radiation ($\lambda = 1.5406 \text{ \AA}$). The XRD patterns were recorded at a scan speed of 1°/min at a step scan of 0.02°. The functional groups present in the samples were studied by Fourier transform infrared spectroscopy (FTIR) employing a KBr pellet method using Perkin-Elmer spectrometer (Perkin Elmer Sdn Bhd, Selangor, Malaysia) equipped with a DTGS finder (USA) by direct scanning in the pan utilizing a fitted universal ATR accessory. The spectra were recorded in the 4000–400 cm⁻¹ range with a resolution of 4 cm⁻¹. The absorption peak height and area were estimated utilizing OMNIC programming variant 1.2a (Nicolet Instrument Corporation, Wisconsin, USA). The Brunauer–Emmett–Teller (BET) surface area of the samples was determined by nitrogen adsorption technique using a Quanta Chrome Nova 1200 Quantachrome Instrument, Florida, USA. The samples were degassed overnight prior to the gas adsorption measurements. The thermal analyses of samples were performed by thermogravimetric analysis using thermo-gravimetric analysis (TGA Q500, TA Instruments, Selangor, Malaysia). The morphology of the samples was examined by scanning electron microscopy (SEM) using EVO 50 (ZEISS, Selangor, Malaysia).

RESULTS AND DISCUSSION

Elemental analysis

Table 1 displays the synthesis parameters, elemental analysis, H/C and O/C ratios, and the yields of HTRW carbon as a function of experimental parameters such as temperature, time and water content.

Table 1 clearly shows that increasing the HTC processing temperature steadily increased the carbon content in the resulting samples with a maximum of 67.3% in the samples processed at 260 °C for 9 h using 40 times more water than the solid wood mass. This apparent improvement in the percentage is due to the effective removal of oxygen and hydrogen. The nitrogen content in the HTRW carbon also increased with processing temperature, which is attributed to the hydrolysis of mainly carbohydrates in the biomass, suggestive of nitrogen incorporation in the carbon matrix. Upon further heat treatment, nitrogen can actually be incorporated in the aromatization/pseudo-graphitization process of the carbon structure.¹⁸ The carbon contents observed in these experiments are similar to the carbon obtained from high cost materials such as cellulose, lignin, sugar, etc. Furthermore, the carbon content from rubber wood using HTC is also better than that from other wood-based biomasses; for example, the carbon content in lignin and cellulose treated at 265 °C for 20 h reaction time were ~68.43% and ~72.1%, respectively.¹⁶ The carbon content in some woody species such as *Cryptomeria japonica* (beluga coal batch) and *Acacia mangium* (asam-asam coal batch) are

Table 1. Synthesis parameters, chemical elemental analysis and product yields for HTRW carbon obtained from the hydrothermal treatment of biomass

	Synthesis conditions			Chemical composition							
	Temperature (°C)	Time (h)	Water ^a (×biomass)	C (wt%)	H (wt%)	N (wt%)	S (wt%)	^b O (wt%)	H/C atomic ratio	O/C atomic ratio	Yield (%)
Rubber wood fiber	Raw (0)	0	0	45.28	6.75	0.56	0.017	47.393	1.78	0.78	100.0
	180	3	20	49.8	6.411	0.61	0.032	43.147	1.53	0.65	87.0
	180	9	20	56.1	6.148	0.63	0.096	37.026	1.31	0.49	83.5
	180	3	40	56.8	6.276	0.65	0.098	36.176	1.32	0.48	91.0
	180	9	40	58.4	6.149	0.66	0.088	34.103	1.25	0.44	89.0
	180	6	30	57.2	6.124	0.65	0.092	35.934	1.27	0.47	90.4
	200	3	20	53.3	6.312	0.62	0.076	39.692	1.41	0.52	79.0
	200	9	20	57.6	6.112	0.66	0.092	35.536	1.26	0.46	75.2
	200	3	40	58.1	6.110	0.67	0.095	35.025	1.25	0.45	82.8
	200	9	40	59.7	5.934	0.68	0.098	33.588	1.184	0.42	80.3
	200	6	30	59.1	6.021	0.68	0.096	34.103	1.21	0.43	81.0
	220	3	20	57.8	6.111	0.66	0.092	35.338	1.26	0.46	70.8
	220	9	20	58.9	6.046	0.67	0.095	34.289	1.22	0.44	66.9
	220	3	40	59.8	5.926	0.68	0.099	33.494	1.18	0.42	74.6
	220	9	40	60.9	5.812	0.89	0.102	32.296	1.14	0.40	72.9
	220	6	30	60.4	5.824	0.88	0.027	32.869	1.15	0.41	73.7
	240	3	20	59.2	6.018	0.90	0.106	33.776	1.21	0.43	64.0
	240	9	20	60.5	5.818	0.90	0.996	31.786	1.15	0.39	60.2
	240	3	40	61.4	5.612	0.92	0.105	31.963	1.09	0.39	68.1
	240	9	40	62.5	5.464	0.95	0.108	30.978	1.04	0.37	66.0
	240	6	30	62.1	5.476	0.94	0.099	31.384	1.05	0.38	66.9
	260	3	20	61.1	5.638	0.94	0.085	32.237	1.10	0.39	56.3
	260	9	20	63.6	5.311	0.95	0.137	30.002	0.99	0.35	53.0
	260	3	40	64.2	5.240	0.98	0.343	29.237	0.97	0.34	60.2
	260	9	40	67.3	5.404	0.97	0.110	26.216	0.96	0.29	58.1
	260	6	30	66.9	5.302	0.95	0.112	26.736	0.94	0.3	59.2

^a Water (times the amount of rubber wood fiber).

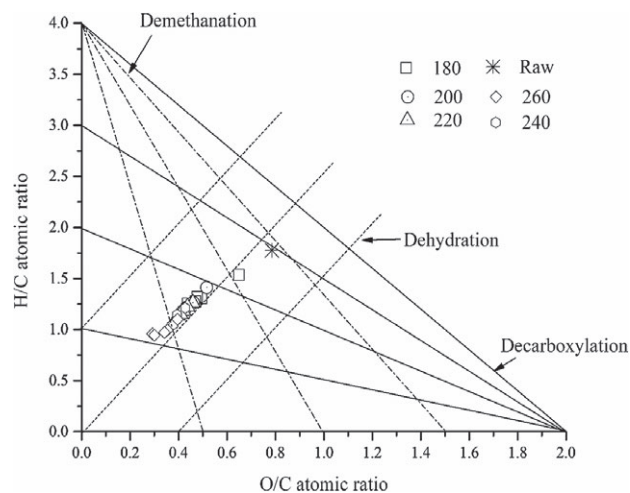
^b O (wt%) = 100 - C (wt%) - H (wt%) - N (wt%) - S (wt%).

reported to be ~68% and ~63.5%, respectively at 300 °C;¹⁸ ~67.3% carbon content in Douglas Fir at 573 K¹⁹ and ~61.6% in pine wood at 300 °C.²⁰ These data show that rubber wood fiber as biomass is a promising and low-cost precursor for carbon synthesis. It was also observed that H/C and O/C ratios decreased when the temperature was raised (from 180 to 260 °C) as shown in Table 1.

The conversion of the biomass to carbon is best represented through the use of a Van Krevelen plot as shown in Fig. 1. This diagram offers a clearer view of the chemical transformation of the HTRW carbon while giving information on the possible reaction taking place during the process involving dehydration and decarboxylation. The improvement in the carbon content and decreasing behaviour of H/C and O/C suggest that decarboxylation and dehydration took place during HTC.^{21,22}

The HTRW carbon yield obtained from the HTC process is in the range 59–87% as shown in Table 1. The maximum yield was at 180 °C; the competitive gasification reduced the yield at higher temperatures.²³ The HTRW carbon yield decreased with further increase in temperature, related to the deoxygenating reactions (e.g. dehydration, decarboxylation) as well as due to evaporation of volatile matter at higher temperatures. Therefore, carbon content percentage and yield have an inverse relationship.

The effect of temperature on HTRW carbon is strong, therefore, it is hard to understand the influence of water and time on the

**Figure 1.** Van Krevelen diagram of raw biomass and HTRW carbon at temperatures 180–260 °C.

carbon content by HTC. Towards this end, the temperature was fixed at ~260 °C but the time and water ratio were varied in the ranges 5–7 h and 25–35 × biomass weight, respectively. The synthesis parameters, elemental analysis of the samples, together

Table 2. Synthesis parameters, elemental composition and product yield

	Synthesis conditions			Chemical composition								
	Temperature (°C)	Sample name	Time (h)	Water ^a (× biomass)	C (wt%)	H (wt%)	N (wt%)	S (wt%)	O ^b (wt%)	H/C atomic ratio	O/C atomic ratio	Yield (%)
Rubber wood fiber	260	T1	5	25	64.95	4.61	0.61	0.19	29.63	0.84	0.34	57.8
		T2	5	35	65.70	4.34	0.63	0.29	29.03	0.79	0.33	61.6
		T3	6	20	63.81	4.72	0.70	0.18	30.58	0.88	0.36	57.1
		T4	6	30	66.53	4.23	0.80	0.36	28.07	0.76	0.32	59.2
		T5	6	40	66.85	4.21	0.92	0.37	27.64	0.75	0.31	58.1
		T6	7	25	65.40	4.34	0.94	0.22	29.08	0.79	0.33	55.3
		T7	7	35	68.10	4.11	1.20	0.43	26.15	0.72	0.29	59.7

^a Water (times of the amount of rubber wood fiber taken).

^b O (wt%) = 100 - C (wt%) - H (wt%) - N (wt%) - S (wt%).

with ratio H/C, ratio O/C and the yields of HTRW carbon during this experiment are shown in Table 2.

The impact of water on the HTC process is not yet clearly understood due to insufficient research. The carbon content increases with time and water content, while the percentage of oxygen decreases. Although the trend is small, it is seen clearly that water and time have an impact on carbon content. The maximum value of carbon content was obtained for ~7 h and a water content of ~35 times. In addition, the hydrogen content decreased slightly while nitrogen and sulphur showed a slight increasing trend.

As shown in the Van Krevelen diagram in Fig. 2, the composition and structures of the chars produced by HTC at 260 °C are clearly different, which demonstrates that the development of the H/C–O/C atomic ratios from raw biomass to HTRW carbon basically follow a dehydration process. The reaction temperature was observed to exhibit the most visible effect on carbon materials. However, the carbonization process was accelerated by water when the temperature was kept constant at 260 °C because water accelerates biomass depolymerization by hydrolysis; the cellulose and hemicellulose are split up into sugar units and the whole biomass structure breaks down rapidly.²⁴ Water is a good heat transfer and storage medium and thus avoids local temperature peaks that might result from exothermal reactions. In sub-critical conditions, the presence of water usually encourages ion-chemistry and suppresses free-radical responses.²⁵ This improves the cleavage-bond of chiefly hydrogen-bonds, especially hydrolysis.

Statistical analysis of HTRW carbon production

Regression analysis was performed to fit the response function with the experimental data. The statistical significance of the second-order model equation was checked by an F-test analysis of variance (ANOVA) via a design of expert (DOE) procedure; the data is shown in Table 3. It can be seen that the Model-F value of carbon is 83.68, which indicates that the model is significant. For a significant model, the prob>F value has to be less than 0.005; but here the generated model has a prob>F value of 0.0001, which indicates that the model is highly significant. The 'Lack of Fit F-value' of 3.75 implies Lack of Fit is not significant relative to the pure error, showing that the model is fitted well.

The regression model is presented in Table S1 in the Supporting information. The regression value of 0.9695 implies that the regression model fits well to the experimental value and it can provide

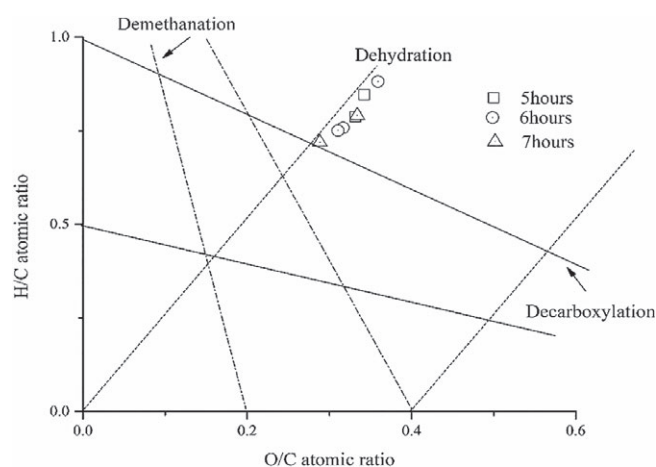


Figure 2. Van Krevelen diagram of HTRW carbon at temperature 260 °C, Water 25–35 times biomass and time 5–7 h.

a useful explanation of the relationships between the independent variables and the response. Equation (1) shows the model obtained using the Design of Expert software.

$$\text{Carbon content (\%)} = +68.58 + 0.798X_2 + 0.78X_1 + 0.491X_2X_1 - 0.29X_2^2 - 0.45X_1^2 \quad (1)$$

where X_1 and X_2 , represent water content and time respectively.

ANOVA was used to check the sufficiency of the second-order model. The statistical properties of the model can be checked by inspecting various diagnostic plots such as plots of actual values obtained from experiments vs predicted values. The correlation between experimental, i.e. actual values of percentage carbon content obtained from the hydrothermal process, and predicted, i.e. theoretical values, are shown in Fig. 3.

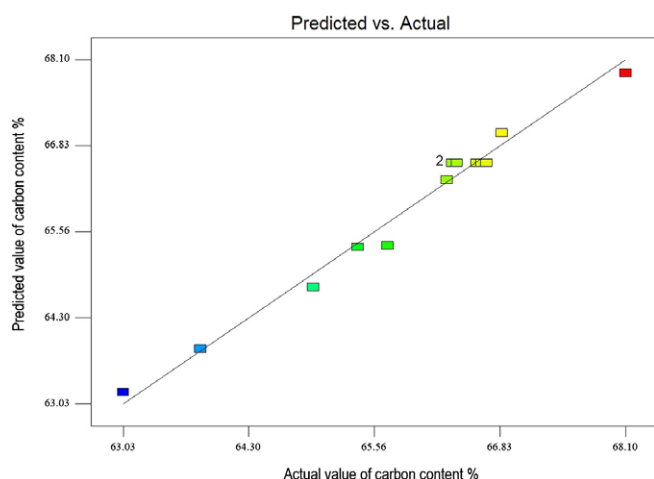
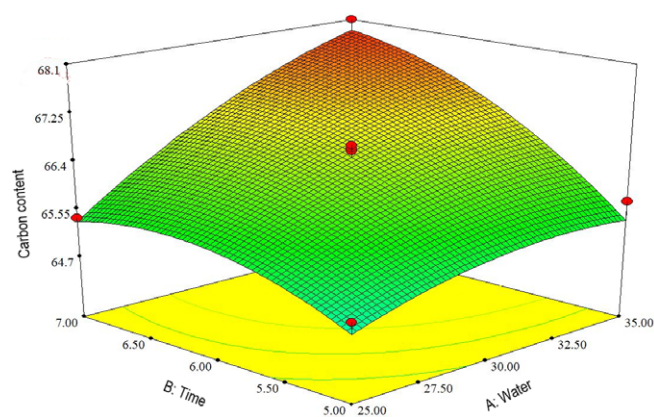
The graph revealed that the proposed model is distinctly adequate and reasonably free from any violation of the independence or constant value assumption. It indicates that the error was evenly distributed and supports the adequacy of the least square fit. These results are well supported by the work done by previous researchers.²⁶

Interaction of water vs time at temperature 260 °C

The interaction between water content and time in the reaction is shown in Fig. 4.

Table 3. Analysis of variance (ANOVA) of the quadratic model for HTRW carbon

Source	Sum of squares	DF	Mean square	F-value	Prob > F	
Model	21.61	5	4.32	83.68	< 0.0001	Significant
A-water	7.57	1	7.57	146.54	< 0.0001	
B-time	7.35	1	7.35	142.27	< 0.0001	
AB	0.95	1	0.95	18.41	0.0027	
A ²	1.98	1	1.98	38.35	0.0003	
B ²	4.95	1	4.95	95.84	< 0.0001	
Residual	3.58	8	0.052			Not significant
Lack of fit	0.29	3	0.095	3.75	0.0943	
Pure error	0.13	5	0.025			
Cor total	22.02	13				

Significant at $p < 0.05$.**Figure 3.** Correlation between the actual and predicted values of percent carbon content.**Figure 4.** 3D plot showing the interaction between time and water content at 260 °C.

The amount of water included has an effect on the product dispersion.²⁷ The water as a solvent has also a pivotal effect on the transportation of fragments out of the network, which keeps these fragments away from the reaction centres. It is discovered that time and water enhance the carbon content. The promising interface of time and water at 260 °C is obtainable by means of

a particular ultimate objective to accomplish maximum carbon content. The carbon content increased at higher water content and at longer reaction times. Water as a solvent plays the vital role of a vigorous transfer medium for ions and moves from one to another bond. Additionally, it constantly breaks as well as connects the latent chemical bonds, and arbitrarily connects them from one compound to another.²⁸ During the HTC procedure, water is vital since it acts as a reactant to redesign the biomass structure. Both a lower and a higher water quantity as well as reaction time have adverse effects on the carbon content percentage. The maximum carbon content, i.e. 68.10% was observed at 35 times water and 7 h time. These results are well supported by Oktaviananda *et al.*²⁹ for HTC of sawdust at different reaction conditions by varying the temperature and biomass–water ratio. The effects of different biomass–water ratios on the hydrothermal treatment process were investigated. For hydrochar, yields were ~63.11%, ~65.67%, ~66.71%, and ~69.57% at biomass water ratio ~5%, ~10%, ~15%, and ~20%, respectively. A high level of interaction was observed between these two parameters.

X-ray diffraction analysis of carbon materials

Figure 5 displays the XRD pattern of raw biomass and powdered HTRW carbon in samples obtained by HTC at 260 °C, time ~5–7 h and water ~25–35 times weight of biomass.

The XRD patterns of raw biomass show two peaks at $2\theta \sim 16.7^\circ$ and $\sim 22.57^\circ$, which were assigned to crystallographic planes. After HTC the patterns show a broad diffraction peak at $2\theta \sim 20\text{--}22^\circ$, a characteristic of disordered carbon.³⁰ As shown in Fig. 5, broad peaks located between 10° and 30° (2θ) for T1, T2, T3, T4, T5, T6, T7 can be ascribed to amorphous carbon^{31,32} and indicate that the corresponding feedstocks have been carbonized as carbon. For raw biomass, there is a sharp crystalline peak, while the HTRW carbon peaks are broad indicating that the crystalline structure was destroyed by HTC, which contained mainly amorphous components.

FTIR analysis

The chemical transformations that occur when the biomass is converted into HTRW carbon by means of hydrothermal carbonization were studied by FTIR. The FTIR spectra of the raw biomass and HTRW carbon obtained at 260 °C, time ~5–7 h and water ~25–35 times weight of biomass are shown in Fig. 6. The FTIR spectra of the hydrochars at 260 °C differs completely from that of the raw biomass as shown in Fig. 6. The spectra conforming to

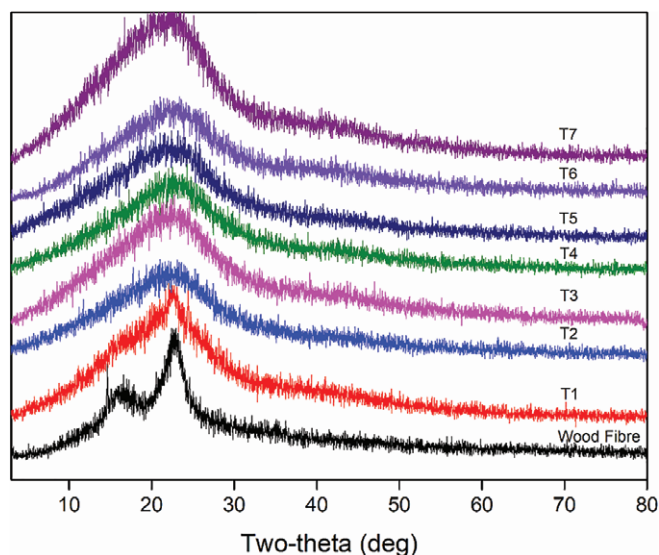


Figure 5. XRD spectra of raw biomass and HTRW carbon produced at 260 °C, water 25–37 times biomass and time 5–7 h.

HTRW carbon samples obtained at 260 °C are very similar and they have several bands which reveal that aromatization processes take place during HTC. The assignment of the peaks in the FTIR spectra are detailed in Table 4.

The vibration at 1620 cm^{-1} shows the presence of aromatic-rings, which is attributed to the C=C vibrations.^{35,36} The HTRW carbon possesses the aliphatic C—H (3000–2800 cm^{-1}) and OH group (3500–3300 cm^{-1}), although the intensity is far less than that of the raw biomass, and in addition the intensity of C—H aliphatic peaks of the HTRW carbon is decreased with respect to temperature. At 1710 cm^{-1} (C=O vibrations corresponding to carbonyl, quinone, ester or carboxyl) and 1000–1460 cm^{-1} (C—O stretching vibrations in hydroxyl, ester or ether and O—H bending vibrations).³⁷ The decrease in the intensity of the bands at 1000–1460 cm^{-1} and the broad band at 3000–3700 cm^{-1} suggest that dehydration occurred during HTC of the raw biomass, endorsing our study of the development of the O/C–H/C atomic ratios based on the Van Krevelen diagram (see Fig. 1).

BET analysis

The surface properties of the HTRW carbon utilized as part of this work were examined by gas adsorption technique. All the HTC samples synthesized at 260 °C, time ~5–7 h and water ~25–35 times weight of biomass showed minor changes in the gas sorption behaviour. This is expected for the sponge like pore framework between the accumulated HTRW carbon. Fine details of the porous texture can be found from the state of the

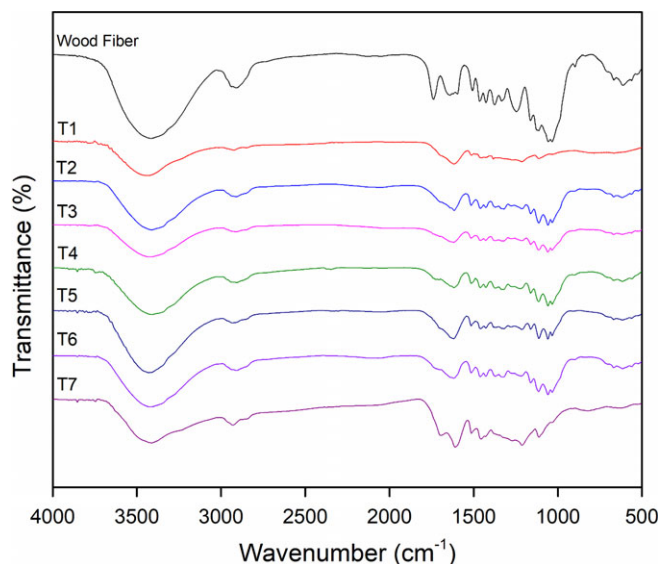


Figure 6. FTIR spectra of raw biomass and HTRW carbon produced at 260 °C, water 25–37 times biomass and time 5–7 h.

N_2 adsorption–desorption isotherms. As per the IUPAC adsorption isotherms classification, the isotherms for HTRW carbon in this investigation indicated qualities that are illustrative of Type II as shown in Fig. S1 in the Supporting information. Besides, macro-porous or non-porous solids are related with Type II isotherm. In this way, the HTRW carbon samples have comparatively small BET surface area because of low porosity as shown in Table 5. In these circumstances, the precise surface area standards merely correspond to the peripheral surface.³⁸ The surface area of the BET obtained from hydrothermal treatment are 10.2, 10.4, 10.2, 10.5, 10.6, 10.3 and 12.1 $\text{m}^2 \text{g}^{-1}$ for the HTRW carbon of samples T1, T2, T3, T4, T5, T6 and T7, respectively. This is supported by earlier studies of biomass-based hydrochars, e.g. Liu *et al.* reported a BET surface area of 21 $\text{m}^2 \text{g}^{-1}$ for pinewood-based hydrochars.²⁰ Titirici *et al.* found BET surface areas of hydrochars as 12, 15.5, and 34 $\text{m}^2 \text{g}^{-1}$ for pine needle, oak leaf, and pine cone respectively.³⁹ The hydrochars derived from banana pseudo-stem and coconut fiber matting had surface areas of 8 and 48 $\text{m}^2 \text{g}^{-1}$, respectively.⁴⁰ The low porosities of carbon or hydrochars have been reported previously by various researchers.^{33,38,41,42}

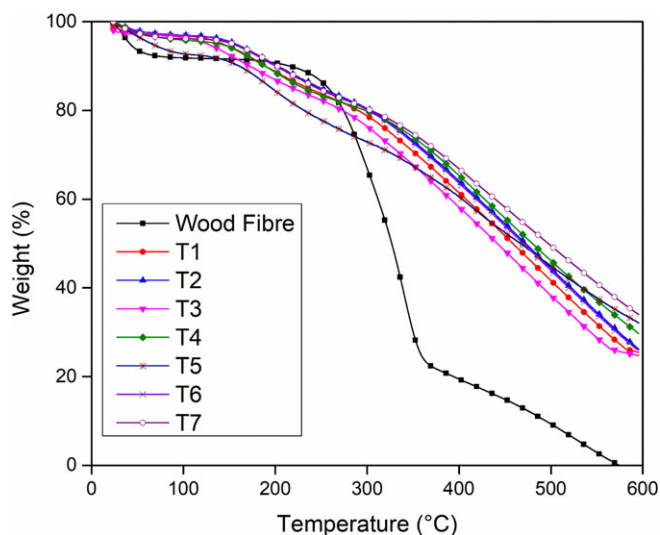
The surface area and pore volume of HTRW carbon at 260 °C, time ~5–7 h and water ~25–35 times weight of biomass are approximately similar for all samples because of the similarity of the synthesis method and material. The measured average BET surface area of the HTRW carbon was ~10.61 $\text{m}^2 \text{g}^{-1}$ with a pore volume ~0.019 $\text{cm}^3 \text{g}^{-1}$. The observed relative lower surface area

Table 4. FTIR peaks observed and assignment of peaks to functional groups using FTIR, adopted from references 33, 34

Wavenumber (cm^{-1})	Functional group	Explanation
1 3700–3000	O—H group	Discover the presence of water, alcohols from cellulose or phenols from lignin
2 3000–2800	C—H group	Little double peaks demonstrating vibrations of the aliphatic C—H bond
3 1800–1650	C=O group	The vibration happens basically from the esters, carboxylic acids or aldehydes from cellulose and lignin
4 1650–1500	C=C group	Vibration from the aromatic rings, existing in lignin
5 1450–1200	C—H bend	Slight peaks of immersion from CH link of aliphatic carbon, methylene, and methyl groups
6 1200–950	C—O group	Vibration from esters, phenols, aliphatic alcohols.
7 900–650	C—H bend	Twisting of CH bond in aromatic compounds

Table 5. Textural parameters of HTRW carbon by HTC synthesis at 260 °C, time ~5–7 h and water ~25–35 times weight of biomass

Material	Temperature (°C)	Time (h)	Water ^a (x biomass)	Surface area (m ² g ⁻¹)	Pore volume (cm ³ g ⁻¹)
Carbon material	260	5	25	10.2	0.0127
		5	35	10.4	0.0106
		6	20	10.2	0.034
		6	30	10.5	0.0185
		6	40	10.6	0.0133
		7	25	10.3	0.0212
		7	35	12.1	0.034

**Figure 7.** TGA curves of raw biomass and HTRW carbon produced at 260 °C, water 25–37 times biomass and time 5–7 h.

is partly contributed by dense particle packing that reduced the porosity.

TGA analysis

The thermal stability of the HTRW carbon samples and raw biomass for comparison were investigated by thermogravimetric analysis (TGA), with results plotted in Fig. 7 as a function of temperature and weight loss on the x and y axis, respectively. The maximum weight loss of all the HTRW carbon produced at 260 °C, time ~5–7 h and water ~25–35 times weight of biomass occurred 440–500 °C compared with raw biomass where the maximum weight loss occurred between 300 and 400 °C. These HTRW carbons seem more resistant to temperature below 300 °C. These results are consistent with previous studies.^{16,43} According to the TG remaining weight, the thermal stability increases with increased reaction temperature and time.^{16,44} The lower volatile matter content and higher fixed carbon content at higher temperatures are possible factors affecting the thermal stability. As shown in Table 6, the TG remaining weight yield is T7 (33.98%) > T5 (32.06%) > T4 (29.71%) > T2 (26.19%) > T6 (26.05%) > T1 (25.48%) > T3 (24.74%). The higher weight yield of HTRW carbon compared with the raw biomass is perhaps linked to the higher ash contents.

The 50% mass loss occurs for raw biomass at 326 °C while for HTRW carbons it occurs at T7 (497 °C) > T4 (480 °C) > T2 (472 °C) > T6 (470 °C) > T5 (467 °C) > T1 (459 °C) > T3 (442 °C) as shown in Table S2 in the Supporting information. Therefore, it is

concluded that at temperature 260 °C, time ~5–7 h and water ~25–35 times weight of biomass, the HTRW carbons produced have better stability than the raw biomass. However, T7 is shown to be the most stable, having 33.98% residue left at 600 °C temperature as shown in Table 6.

SEM analysis

Figure 8 shows the SEM spectra of raw biomass (Fig. 8(a)) and HTRW carbon obtained from hydrothermal treatment at 260 °C (Fig. 8(b), water ~35 times and time ~7 h, Fig. 8(c), water ~40 times and time ~6 h, Fig. 8(d), water ~35 times and time ~7 h). It should be noted that the HTRW carbon except raw biomass exhibits a similar morphology and comprises mostly of aggregates of micro-spheres with a diameter of 1.5–5 μm. This confirms the effect that hydrothermal action has on the structure of HTRW carbon.³³

There is major transformation seen in Fig. 8(a–d) and no major changes noticed on the structures of the hydrochars at a temperature of 260 °C. The surface topography of HTRW carbons (T2, T5 and T7) retains the spherical appearance. However, unlike T5 and T7, T2 has few microspheres but many cracks. Although the fibers start to break the pore size of the surfaces of the HTRW carbon were seen to increase in surface area as water content and time were increased. Furthermore, the development of small globules was discovered in the micro-fibrils area of the HTRW carbon.

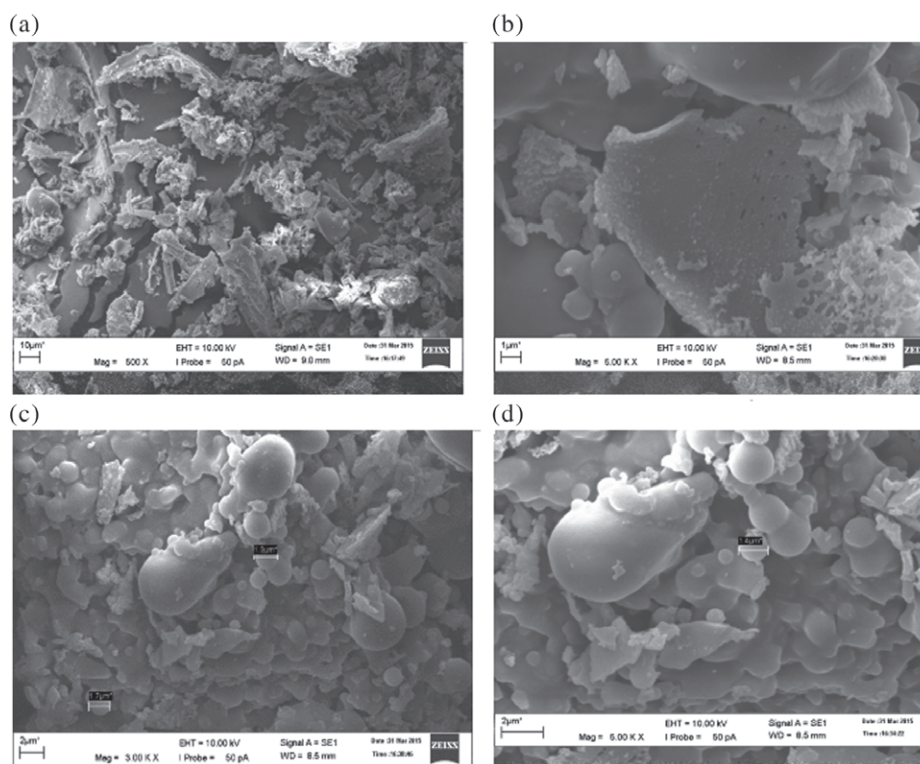
Proposed mechanism of the hydrothermal carbonization (HTC) process

The rate of reaction during the HTC procedure is not broadly known due to the inadequate research in this area.¹¹ The reaction procedure was anticipated to be in three phases: hydrolysis, dehydration or decarboxylation, and carbonization through polymerization and aromatization processes. Figure 9 shows schematically the proposed mechanism.

The water performs as both reactant and catalyst in the HTC process during the hydrolysis reaction.⁴⁵ The carbonization of biomass is accelerated by the presence of water, which also affects the product distribution. At the same time, the water in the biomass functions not only as reacting medium but also as reactant.⁴⁶ It is suggested that HTC accelerates the de-polymerization of rubber wood fibers by a hydrolysis process, which occurs when the hydronium ions from the auto-ionization of water act as catalysts.⁴⁷ Compared with the ambient water, the dielectric constant of pressurized hot water is decreased by the increased temperature²⁶ and it serves to increase the solubility as well as rate of reaction in organic-compounds. Simultaneously, the ionization constant of the water is increased by increasing the temperature and is increased by three orders of magnitude over that of

Table 6. Thermal properties of raw biomass and HTRW carbon produced at 260 °C, time ~5–7 h and water ~25–35 times weight of biomass

Sample	Residue left at different temperature (%)					
	100 °C	200 °C	300 °C	400 °C	500 °C	600 °C
Wood fiber	91.84	90.74	66.83	19.45	9.33	0.0
T1	96.79	88.77	78.79	61.43	41.62	25.48
T2	96.94	90.35	80.39	64.07	44.42	26.19
T3	96.55	86.94	76.36	58.2	38.3	24.74
T4	95.87	88.61	79.8	65.3	46.14	29.71
T5	92.77	84.43	72.89	60.5	44.97	32.06
T6	96.95	90.02	80.18	63.6	43.9	26.05
T7	96.17	90.3	80.38	66.83	49.48	33.98


Figure 8. SEM images of wood fiber and T2, T5, T7 derived HTRW carbon.

ambient water.⁴⁸ OH ions as well as H⁺ are produced as shown in the FTIR analysis (Table 3); hence, H⁺ ions can act as catalysts in the hydrolysis reaction of rubber wood, which enables the lower decomposition temperature of biomass under HTC. Rubber wood comprises cellulose, hemicellulose and lignin as shown in Fig. 9. The hemicellulose is prone to hydrolysis at temperatures below 200 °C through hydrothermal reaction. The fractional bonds of glycosidic cellulose are cracked between of 200 and 220 °C in an acidic medium.⁴⁹ It has been found also that the decomposition of cellulose (glucose/oligomers) starts at 200 °C temperature, with a short reaction time.⁵⁰ Simultaneously the soluble lignin remains fragmented and is dissolved by increasing the reaction time. The distinctive products of cellulose, hemicellulose and lignin were 5-HMF, furfural as well as phenolic by-products, respectively as confirmed by FTIR wavenumbers (1200–950 cm⁻¹). The furfural compounds remain susceptible to condensation reaction associated with hydrolytic ring opening below acidic media.⁵¹ In addition, a few polymerization HTRW carbon micro-spheres

were acquired via polymerization/oligomerization and condensation reaction of furfural by-products at the surface of fibers via homogeneous water solvable reactions. Study of hydrothermal reactions with straw biomass have been reported by Ibbett *et al.*⁵² and they stated that the degradation of hemicellulose starts above 195 °C temperature. The partial amorphous cellulose was split into lesser molecules, and the 5 HMF was the key typical degradation outcome of these molecules, that forms hydrochar microspheres by the same process as furfural through hydrothermal reaction and these results are also conformed by Sevilla.³³ Instead of the non-dissolving cellulose, the processes of reactions resemble the pyrolysis procedure by means of intra-molecular organization, dehydration as well as decarboxylation reaction to make a connected porous complex structure. Some of the lignins remained disjointed, disseminated as well as softened in the liquid stage at temperature 200 °C by a prolonged reaction period. Moreover, the dissolving procedure of lignins is controlled by

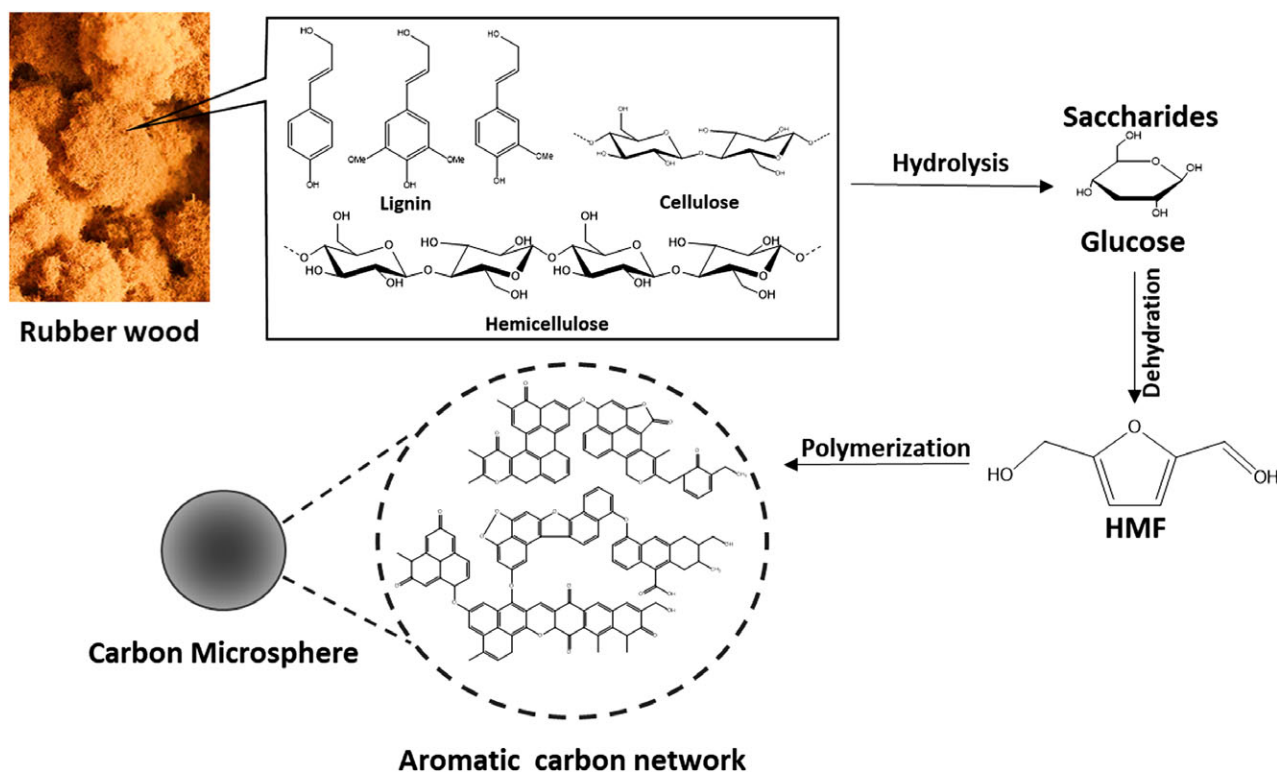


Figure 9. Proposed mechanism for formation of spherical-like structure HTRW carbon from rubber wood by hydrothermal carbonization.

diffusion, and a lengthier reaction time can lead to improved solubility of lignins. In addition the soluble lignins were consistently hydrolyzed as well as decayed to the by-products of phenols,⁵³ which forms microsphere HTRW carbon by re-polymerization using other water solvable compounds. Furthermore, the undissolved lignin too follows a similar undissolved cellulose reaction process. Therefore, 5-HMF, furfurals as well as phenolic by-products continued to be polymerized or condensed to microspheres in addition to the number as well as the size of the spheres progressively increases with respect to reaction period, which is well backed by the SEM study. Furthermore, the primary structural network of non-dissolved lignin as well as cellulose was just about disrupted completely as well as experiencing a heterogeneous pyrolysis-type procedure then formed an interconnected porous-network structures named aromatic carbon network.

CONCLUSIONS

This work demonstrates that rubber wood could be an excellent low-cost precursor for synthesis of carbon. An optimum condition to obtain HTRW carbon with carbon content as high as ~68% was developed; hydrothermal carbonization temperature of ~260 °C for 7 h with 35 times more water than solid biomass. Our experiments demonstrate that, apart from temperature, the amount of water with respect to the woody biomass and the duration of reaction also play an important role in the HTC process. The higher temperatures generally accelerate the hydrothermal carbonization of biomass, resulting in higher carbon content of HTRW carbon but low yields. The H/C and O/C ratio of HTRW carbon are observed to have large differences with respect to the starting material. The FTIR studies verify that improved carbon content is due to removal of oxygen and water during HTC;

and SEM analysis demonstrates that the HTC carbon is spherical, with the number and size of spheres progressively increasing with reaction time. A mechanism is proposed here for the formation of HTRW carbon from rubber wood, which follows the order: (i) hydrolysis of biomass (rubber wood fiber) chain; (ii) dehydration into soluble products of the monomers that come from the hydrolysis of biomass; (iii) polymerization of the soluble products; (iv) aromatization of the polymers thus formed an interconnected porous network structure called the aromatic carbon network.

ACKNOWLEDGEMENTS

The authors thank the Laboratory of Adhesion & Bio-Composites, Seoul National University, Seoul, Republic of Korea and University Malaysia Pahang for funding to complete this research. RJ acknowledges the Flagship Leap 3 (RDU172201) of Universiti Malaysia Pahang.

Supporting Information

Supporting information may be found in the online version of this article.

REFERENCES

- 1 BIROL F, *IEA World Energy Outlook 2006*. International Energy Agency–Economic Analysis Division, Paris, p. 37 (2006).
- 2 Mierzejewska J, Dąbkowska K, Chreptowicz K and Sokółowska A, Hydrolyzed corn stover as a promising feedstock for 2-phenylethanol production by non-conventional yeast. *J Chem Technol Biotechnol* (2018).
- 3 Yeh TM, Dickinson JG, Franck A, Linic S, Thompson LT Jr and Savage PE, Hydrothermal catalytic production of fuels and chemicals from aquatic biomass. *J Chem Technol Biotechnol* **88**:13–24 (2013).
- 4 Misnon II, Zain NKM, Aziz RA, Vidyadharan B and Jose R, Electrochemical properties of carbon from oil palm kernel shell for high performance supercapacitors. *Electrochim Acta* **174**:78–86 (2015).

- 5 Ro KS, Cantrell KB and Hunt PG, High-temperature pyrolysis of blended animal manures for producing renewable energy and value-added biochar. *Ind Eng Chem Res* **49**:10125–10131 (2010).
- 6 Kang S, Li X, Fan J and Chang J, Solid fuel production by hydrothermal carbonization of black liquor. *Bioresour Technol* **110**:715–718 (2012).
- 7 Lehmann J, A handful of carbon. *Nature* **447**:143–144 (2007).
- 8 Vaccari F, Baronti S, Lugato E, Genesio L, Castaldi S, Fornasier F *et al.*, Biochar as a strategy to sequester carbon and increase yield in durum wheat. *Eur J Agron* **34**:231–238 (2011).
- 9 Erdogan E, Atila B, Mumme J, Reza MT, Toptas A, Elibol M *et al.*, Characterization of products from hydrothermal carbonization of orange pomace including anaerobic digestibility of process liquor. *Bioresour Technol* **196**:35–42 (2015).
- 10 Benavente V, Calabuig E and Fullana A, Upgrading of moist agro-industrial wastes by hydrothermal carbonization. *J Anal Appl Pyrolysis* **113**:89–98 (2015).
- 11 Funke A and Ziegler F, Hydrothermal carbonization of biomass: a summary and discussion of chemical mechanisms for process engineering. *Biofuels Bioprod Biorefin* **4**:160–177 (2010).
- 12 Jamari SS and Howse JR, The effect of the hydrothermal carbonization process on palm oil empty fruit bunch. *Biomass Bioenergy* **47**:82–90 (2012).
- 13 Xiao L-P, Shi Z-J, Xu F and Sun R-C, Hydrothermal carbonization of lignocellulosic biomass. *Bioresour Technol* **118**:619–623 (2012).
- 14 Zhu Z, Liu Z, Zhang Y, Li B, Lu H, Duan N *et al.*, Recovery of reducing sugars and volatile fatty acids from cornstarch at different hydrothermal treatment severity. *Bioresour Technol* **199**:220–227 (2016).
- 15 Hu B, Wang K, Wu L, Yu SH, Antonietti M and Titirici MM, Engineering carbon materials from the hydrothermal carbonization process of biomass. *Adv Mater* **22**:813–828 (2010).
- 16 Kang S, Li X, Fan J and Chang J, Characterization of hydrochars produced by hydrothermal carbonization of lignin, cellulose, D-xylose, and wood meal. *Ind Eng Chem Res* **51**:9023–9031 (2012).
- 17 Deraman M, Zakaria S, Husin M, Aziz A, Ramli R, Mokhtar A *et al.*, X-ray diffraction studies on fiber of oil palm empty fruit bunch and rubberwood for medium-density fiberboard. *J Mater Sci Lett* **18**:249–253 (1999).
- 18 Nonaka M, Hirajima T and Sasaki K, Upgrading of low rank coal and woody biomass mixture by hydrothermal treatment. *Fuel* **90**:2578–2584 (2011).
- 19 Kobayashi N, Okada N, Hirakawa A, Sato T, Kobayashi J, Hatano S *et al.*, Characteristics of solid residues obtained from hot-compressed-water treatment of woody biomass. *Ind Eng Chem Res* **48**:373–379 (2008).
- 20 Liu Z, Zhang F-S and Wu J, Characterization and application of chars produced from pinewood pyrolysis and hydrothermal treatment. *Fuel* **89**:510–514 (2010).
- 21 Sevilla M, Maciá-Agullo JA and Fuertes AB, Hydrothermal carbonization of biomass as a route for the sequestration of CO₂: chemical and structural properties of the carbonized products. *Biomass Bioenergy* **35**:3152–3159 (2011).
- 22 Berge ND, Ro KS, Mao J, Flora JR, Chappell MA and Bae S, Hydrothermal carbonization of municipal waste streams. *Environ Sci Technol* **45**:5696–5703 (2011).
- 23 Yang H, Yan R, Chen H, Lee DH and Zheng C, Characteristics of hemicellulose, cellulose and lignin pyrolysis. *Fuel* **86**:1781–1788 (2007).
- 24 Kruse A, Supercritical water gasification. *Biofuels Bioprod Biorefin* **2**:415–437 (2008).
- 25 Yu S-H, Cui X, Li L, Li K, Yu B, Antonietti M *et al.*, From starch to metal/carbon hybrid nanostructures: hydrothermal metal-catalyzed carbonization. *Adv Mater* **16**:1636–1640 (2004).
- 26 Nizamuddin S, Mubarak N, Tiripathi M, Jayakumar N, Sahu J and Ganesan P, Chemical, dielectric and structural characterization of optimized hydrochar produced from hydrothermal carbonization of palm shell. *Fuel* **163**:88–97 (2016).
- 27 Behar F, Lewan M, Lorant F and Vandenbroucke M, Comparison of artificial maturation of lignite in hydrous and nonhydrous conditions. *Org Geochem* **34**:575–600 (2003).
- 28 Mahoney N, *The Chemistry of Water*. Special Report of National Science Foundation, Virginia (2005).
- 29 Oktaviananda C, Rahmawati RF, Prasetya A, Purnomo CW, Yuliansyah AT and Cahyono RB eds, Effect of temperature and biomass-water ratio to yield and product characteristics of hydrothermal treatment of biomass, in *AIP Conference Proceedings*. AIP Publishing, New York (2017).
- 30 Banwell CN and EM MC, *Fundamentals of Molecular Spectroscopy*. Tata McGraw-Hill, New Delhi (2006).
- 31 Wu X, Zhu W, Zhang X, Chen T and Frost RL, Catalytic deposition of nanocarbon onto palygorskite and its adsorption of phenol. *Appl Clay Sci* **52**:400–406 (2011).
- 32 Xie Z-L, White RJ, Weber J, Taubert A and Titirici MM, Hierarchical porous carbonaceous materials via ionothermal carbonization of carbohydrates. *J Mater Chem* **21**:7434–7442 (2011).
- 33 Sevilla M and Fuertes AB, The production of carbon materials by hydrothermal carbonization of cellulose. *Carbon* **47**:2281–2289 (2009).
- 34 Sundqvist B, Karlsson O and Westermark U, Determination of formic-acid and acetic acid concentrations formed during hydrothermal treatment of birch wood and its relation to colour, strength and hardness. *Wood Sci Technol* **40**:549–561 (2006).
- 35 Sun X and Li Y, Colloidal carbon spheres and their core/shell structures with noble-metal nanoparticles. *Angew Chem Int Ed* **43**:597–601 (2004).
- 36 Holgate HR, Meyer JC and Tester JW, Glucose hydrolysis and oxidation in supercritical water. *AIChE J* **41**:637–648 (1995).
- 37 Kabyemela BM, Adschiri T, Malaluan RM and Arai K, Glucose and fructose decomposition in subcritical and supercritical water: detailed reaction pathway, mechanisms, and kinetics. *Ind Eng Chem Res* **38**:2888–2895 (1999).
- 38 Fuertes A, Arbertain MC, Sevilla M, Maciá-Agulló JA, Fiol S, López R *et al.*, Chemical and structural properties of carbonaceous products obtained by pyrolysis and hydrothermal carbonisation of corn stover. *Soil Res* **48**:618–626 (2010).
- 39 Titirici MM, Thomas A, Yu S-H, Müller J-O and Antonietti M, A direct synthesis of mesoporous carbons with bicontinuous pore morphology from crude plant material by hydrothermal carbonization. *Chem Mater* **19**:4205–4212 (2007).
- 40 Romero-Anaya A, Lillo-Ródenas M, De Lecea CS-M and Linares-Solano A, Hydrothermal and conventional H₃PO₄ activation of two natural bio-fibers. *Carbon* **50**:3158–3169 (2012).
- 41 Sevilla M and Fuertes AB, Chemical and structural properties of carbonaceous products obtained by hydrothermal carbonization of saccharides. *Chem-Eur J* **15**:4195–4203 (2009).
- 42 Parshetti GK, Hoekman SK and Balasubramanian R, Chemical, structural and combustion characteristics of carbonaceous products obtained by hydrothermal carbonization of palm empty fruit bunches. *Bioresour Technol* **135**:683–689 (2013).
- 43 Aydinçak K, Tr Y, Sinağ A and Esen B, Synthesis and characterization of carbonaceous materials from saccharides (glucose and lactose) and two waste biomasses by hydrothermal carbonization. *Ind Eng Chem Res* **51**:9145–9152 (2012).
- 44 Nizamuddin S, Jayakumar NS, Sahu JN, Ganesan P, Bhutto AW and Mubarak NM, Hydrothermal carbonization of oil palm shell. *Korean J Chem Eng* **32**:1789–1797 (2015).
- 45 Toor SS, Rosendahl L and Rudolf A, Hydrothermal liquefaction of biomass: a review of subcritical water technologies. *Energy* **36**:2328–2342 (2011).
- 46 Nizamuddin S, Baloch HA, Griffin G, Mubarak N, Bhutto AW, Abro R *et al.*, An overview of effect of process parameters on hydrothermal carbonization of biomass. *Renew Sustain Energy Rev* **73**:1289–1299 (2017).
- 47 Sabzoi N, Yong E, Jayakumar N, Sahu J, Ganesan P, Mubarak N *et al.*, An optimisation study for catalytic hydrolysis of oil palm shell using response surface methodology. *J Oil Palm Res* **27**:339–351 (2015).
- 48 Brunner G, Near critical and supercritical water. Part I. Hydrolytic and hydrothermal processes. *J Supercrit Fluids* **47**:373–381 (2009).
- 49 Behrendt F, Neubauer Y, Oevermann M, Wilmes B and Zobel N, Direct liquefaction of biomass. *Chem Eng Technol* **31**:667–677 (2008).
- 50 Minowa T, Zhen F and Ogi T, Cellulose decomposition in hot-compressed water with alkali or nickel catalyst. *J Supercrit Fluids* **13**:253–259 (1998).
- 51 Mariscal R, Maireles-Torres P, Ojeda M, Sádaba I and Granados ML, Furfural: a renewable and versatile platform molecule for the synthesis of chemicals and fuels. *Energy Environ Sci* **9**:1144–1189 (2016).
- 52 Ibbett R, Gaddipati S, Davies S, Hill S and Tucker G, The mechanisms of hydrothermal deconstruction of lignocellulose: new insights from thermal–analytical and complementary studies. *Bioresour Technol* **102**:9272–9278 (2011).
- 53 Hashaikeh R, Fang Z, Butler I, Hawari J and Kozinski J, Hydrothermal dissolution of willow in hot compressed water as a model for biomass conversion. *Fuel* **86**:1614–1622 (2007).